

Field-free molecular orientation by THz laser pulses at high temperature

M. Lapert* and D. Sugny†

July 13, 2012

Abstract

We investigate to which extent a THz laser pulse can be used to produce field-free molecular orientation at high temperature. We consider laser pulses that can be implemented with the state of the art technology and we show that the efficiency of the control scheme crucially depends on the parameters of the molecule. We analyze the temperature effects on molecular dynamics and we demonstrate that, for some molecules, a noticeable orientation can be achieved at high temperature.

1 Introduction

Manipulating the molecular rotational degree of freedom remains a goal of primary interest in photochemistry with applications extending from chemical reactivity to nanoscale design [1, 2, 3]. In this framework, molecular alignment and orientation constitute a well-established topic both from the experimental and theoretical points of view [4, 5]. While the alignment process is now well understood in the adiabatic [6] or sudden regime [7] with recent extensions such as the molecular classical rotation [8], the deflection of aligned molecules [9], the planar alignment [10, 11, 12] or the analysis of the dissipation effects [13, 14], work remains to be done in order to control and produce molecular orientation with a sufficient high efficiency. On the theoretical side, several basic mechanisms have been proposed, built on intuitive or optimal control strategies [15, 16]. Among others, we can cite the kick mechanism which consists in a sudden impact to the molecule by a half-cycle pulse (HCP) [17, 18, 19, 20, 21, 22], its combination with a laser field [23, 24, 25] or the $(\omega - 2\omega)$ scheme [26, 27, 28, 29, 30, 31, 32, 33]. Due to the efficiency of the first process based on its asymmetric temporal shape, most of the theoretical works have focused on its application [34, 35, 36, 37, 38]. However, recent studies [39, 40] have pointed out the inherent experimental difficulties associated to the use of such pulses, which are distorted when they propagate in free space as well as through focusing optics [41]. This phenomenon, due to the DC component of the field, makes thus problematic the experimental implementation of these techniques in the control of molecular rotation. In

*Institut für Quanteninformationsverarbeitung, Universität Ulm, D-89069 Ulm, GERMANY

†Laboratoire Interdisciplinaire Carnot de Bourgogne (ICB), UMR 5209 CNRS-Université de Bourgogne, 9 Av. A. Savary, BP 47 870, F-21078 DIJON Cedex, FRANCE, dominique.sugny@u-bourgogne.fr

this framework, a fundamental question is whether it is possible to orient linear molecules in the THz regime by using only zero area laser pulses. These latter do not contain DC field and are therefore free of these propagation distortions. This problem has been recently addressed theoretically [40, 42, 43, 44, 45] and experimentally [46], but no systematic study of the efficiency of this process has been done. Note that this question is not trivial since the sudden impact approximation predicts no post-pulse orientation in this regime [19, 20, 40]. We present in this paper a complete analysis of this control strategy by considering different linear molecules. We establish under which conditions this process is efficient and we analyze its robustness with respect to temperature effects. Two mechanisms leading to molecular orientation are identified. The first one is valid at low temperature, while the second process is only efficient for higher temperatures. In this second non-intuitive control scheme, we show the positive role of temperature effects in the orientation mechanism.

The paper is organized as follows. The model system is presented in Sec. 2. The different numerical results are discussed in Sec. 3. Conclusions and prospective views are given in Sec. 4.

2 The model system

We consider the control of a linear polar molecule by a linearly polarized THz laser field $E(t)$ of zero area. The molecule is assumed to be in its ground vibronic state. Within the rigid rotor approximation, the Hamiltonian of the system can be written as

$$H(t) = BJ^2 - \mu_0 E(t) \cos \theta, \quad (1)$$

where B is the rotational constant, J^2 the angular momentum operator and μ_0 the permanent dipolar moment. We neglect in this paper the effect of the polarizability components since the maximum intensity of the electric field remains moderate. The units used throughout the paper are atomic units unless otherwise specified. At non zero temperature, the system can be either described by a density matrix $\rho(t)$ with a dynamics governed by the von Neumann equation

$$i \frac{\partial \rho(t)}{\partial t} = [H(t), \rho(t)], \quad (2)$$

where $\rho(0)$ is the canonical density operator at thermal equilibrium, or by a set of wave functions $|\psi_{J_0, M_0}(t)\rangle$ satisfying each the Schrödinger equation:

$$i \frac{\partial |\psi_{J_0, M_0}\rangle}{\partial t} = H(t) |\psi_{J_0, M_0}\rangle, \quad (3)$$

with as initial state $|\psi_{J_0, M_0}(t=0)\rangle = |J_0, M_0\rangle$. The second representation given by Eq. (3), which is more suited to the control mechanisms interpretation, will be used in this work. The expectation value $\langle \cos \theta \rangle$ defined by

$$\langle \cos \theta \rangle(t) = \frac{1}{Z} \sum_{J_0=0}^{+\infty} c_{J_0} \sum_{M_0=-J_0}^{M_0=J_0} \langle \psi_{J_0, M_0} | \cos \theta | \psi_{J_0, M_0} \rangle, \quad (4)$$

is taken as a quantitative measure of orientation, with the weights $c_J = e^{-BJ(J+1)/(k_B T)}$ and the partition function $Z = \sum_{J=0}^{\infty} \sum_{M=-J}^J c_J$, where T is the temperature

Table 1: Molecular parameters of different molecules used in the numerical computations. Numerical values are taken to be $E_0 = 2.19$ MV/cm, $\delta = 5$ ps and $f = 0.5$ THz.

Molecule	OCS	HF	LiH	CO	LiCl
B (cm ⁻¹)	0.2029	20.956	7.513	1.931	1.345
μ_0 (debye)	0.712	1.820	5.88	0.112	6.33
A	117.8497	2.9167	26.2842	1.9479	158.0563
F	13.0823	0.1267	0.3533	1.3746	1.9735
D	0.1911	19.7371	7.0760	1.8187	1.2668

and k_B the Boltzman constant. In the rest of the paper, we will need to separate the zero temperature contribution to the thermal one, which are respectively denoted by $\langle \cos \theta \rangle_0$ and $\langle \cos \theta \rangle_T$. In the zero temperature response, the sum of Eq. (4) is carried out only for $J_0 = 0$, while for the thermal contribution, the expectation value is computed over the other values of J_0 .

The electric field is assumed to be of the form

$$E(t) = E_0 f(t) = E_0 \cos^2\left(\pi \frac{t}{\delta}\right) \sin(2\pi f t), \quad t \in [-\delta/2, \delta/2],$$

$$E(t) = 0 \quad \text{otherwise,}$$

where E_0 is the amplitude of the pulse, δ its duration and f its central frequency. By symmetry, this field has a zero area for any values of δ and f . Note that the sudden impact approximation can be applied if the pulse duration δ is small with respect to the rotational period $T_{\text{per}} = \pi/B$. This also means that noticeable orientation can be produced only for sufficient large values of δ [19, 40].

The Schrödinger equation (3) can be written as

$$i \frac{\partial |\psi_{J_0, M_0}\rangle}{\partial \tau} = [J^2 - A \cos \theta f(\tau)] |\psi_{J_0, M_0}\rangle, \quad (5)$$

where the new dimensionless parameters are defined by:

$$\tau = Bt, \quad A = \frac{\mu_0 E_0}{B}, \quad F = \frac{f}{B}, \quad D = B\delta, \quad \tilde{T} = \frac{Tk_B}{B},$$

with $f(\tau) = \cos^2(\pi \frac{\tau}{D}) \sin(2\pi F \tau)$. In these coordinates, the rotational period becomes $T_{\text{per}} = \pi$ and the pulse duration is D . These effective parameters completely describe the dynamical evolution of the system and the degree of molecular orientation produced. They will give a general understanding of the orientation mechanism free of any particular molecule. Note that the rotational constant B is a crucial parameter in these new coordinates since the effective field, frequency and duration (A, F, D) depend on B . For numerical applications, we will consider the parameters listed in Table 1.

3 Numerical Results

We begin our study by a general analysis of the maximum degree of orientation that can be reached as a function of the rotational constant B and the temperature T . A fictive molecule with a permanent dipolar moment of 1 debye has been

considered in the computation. The field amplitude is assumed to be $E_0 = 2.19$ MV/cm (i.e. with a peak amplitude of 2 MV/cm), which corresponds roughly to the maximum amplitude of THz pulses actually available experimentally [47]. This dependance is shown in Fig. 1 where two zones of high orientation can be clearly distinguished: an upper zone, denoted (I), associated to high values of B and low temperature and a flat zone, denoted (II) requiring small rotational constants and larger temperatures up to 250 K. If the rotational constant is

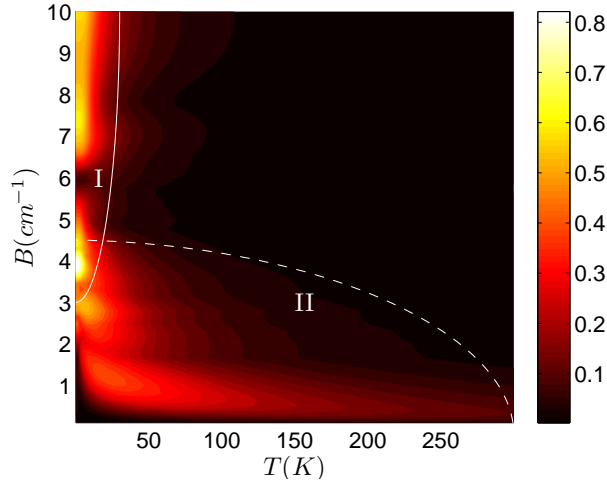


Figure 1: (Color online) Maximum orientation as a function of the rotational constant B and the temperature T . The field parameters are $\delta = 5$ ps, $f = 0.5$ THz and $E_0 = 2.19$ MV/cm. Two regions (I) and (II) of the diagram are delimited by arcs of ellipses.

lower than 2 cm^{-1} , we first notice that a very weak orientation is produced at $T = 0$ K. The rotational period varying as the inverse of B , this result can be explained through the sudden impact approximation [19, 20, 40]. Another standard feature shown in previous studies is the detrimental effect of temperature on molecular orientation [5, 19, 20]. This behavior can be recovered in the case of region (I) where almost no orientation is obtained for a temperature larger than 100 K. By comparison, the orientation observed in zone (II) is rather unexpected, since the temperature effect becomes positive, no orientation being produced at very low temperature. One of the goal of this work will be to explore the basic mechanism at the origin of this non trivial phenomenon.

The orientation mechanism.

We first present a general spectral analysis of the control problem. We use in the following the dimensionless coordinates introduced in Sec. 2, for which the molecular spectrum is a discrete spectrum composed of the frequencies $\omega_J = 2(J + 1)$. To simplify the discussion, we associate to each frequency a weight P which is defined as the average of the initial thermal population of the levels J and $J + 1$, i.e. $P = (c_J + c_{J+1})/2$. The spectrum of the control field is proportional to the one of the function $f(\tau)$ and can roughly be approximated by a gaussian spectrum centered at $\nu = F$ with a bandwidth proportional to $1/D$. Different spectra are represented in Fig. 2 and 3 for different values of D

and F , respectively. In the case of Fig. 2, only the width of the field spectrum is changed, while only the central frequency is modified in Fig. 3. From a qualitative point of view, the overlap between the molecular and the field spectra is a necessary condition to produce molecular orientation. Figure 2 displays two cases with different values of D , i.e. a pulse with a large spectrum overlapping many transitions including the first one, and a pulse with a larger width D corresponding to a narrower spectrum. The first pulse can produce orientation at zero and non-zero temperatures, while the second one is only efficient at non zero temperature. This behavior is confirmed in the top panel of Fig. 4. Figure 3 depicts two different situations, a first one with a low main frequency which overlaps with the first frequency spectrum and a second case where the main frequency is far from the first molecular transition. The first pulse should work at zero and nonzero temperatures due to the overlap with other transitions while in the second example, we cannot expect orientation at zero temperature but only for $\tilde{T} \neq 0$. The corresponding orientation responses are given in the bottom panel of Fig. 4. Comparing in Fig. 4 the efficiency of the pulses of Fig. 2 and 3, one observes that at $\tilde{T} \neq 0$, a stronger orientation is obtained in the first case of Fig. 2 due to a larger overlap of the field spectrum with the population distribution. In other words, a noticeable orientation is produced only for a large bandwidth of the laser field.

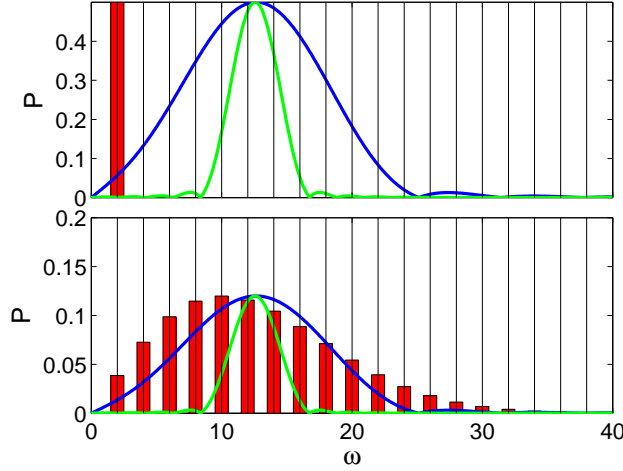


Figure 2: (Color online) Plot of the spectral distribution of the field at $\tilde{T} = 0$ and $\tilde{T} = 50$ ($T = 143.9$ K for $B = 2$ cm $^{-1}$) on the top and bottom panels, respectively. The amplitude of the field spectrum is arbitrary. Control fields parameters are taken to be $D = 1$ ($\delta = 2.654$ ps for $B = 2$ cm $^{-1}$) for the blue (black) line and $D = 3$ ($\delta = 7.963$ ps for $B = 2$ cm $^{-1}$) for the green (gray) line. Other parameters are fixed to $F = 2$ ($f = 0.753$ THz for $B = 2$ cm $^{-1}$) and $A = 4$. The columns represent the population distribution $P = (c_J + c_{J+1})/2$ at the corresponding frequency $\omega = 2(J + 1)$. The quantities P and ω are unitless.

The interpretation of the previous results leads to two basic mechanisms governing the orientation response. The orientation created at $T \simeq 0$ K can be associated to a rotational ladder climbing mechanism from the ground energy

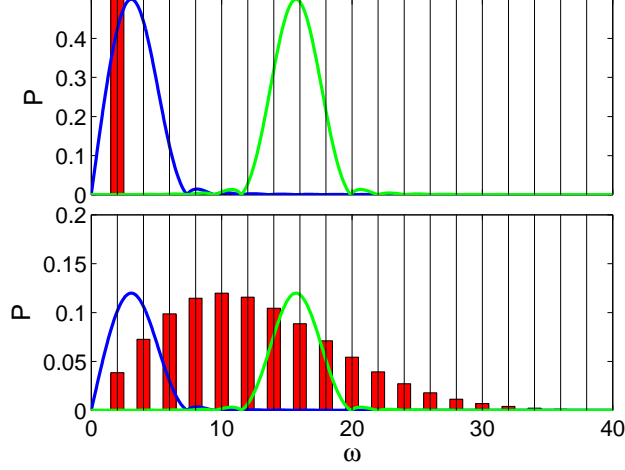


Figure 3: (Color online) Same as Fig. 2 but for $F = 0.5$ ($f_1 = 0.188$ THz for $B = 2$ cm $^{-1}$) in blue or dark and $F = 2.5$ ($f = 0.942$ THz for $B = 2$ cm $^{-1}$) in green or gray. The other parameters are given by $D = 3$ ($\delta = 7.96$ ps for $B = 2$ cm $^{-1}$) and $A = 4$.

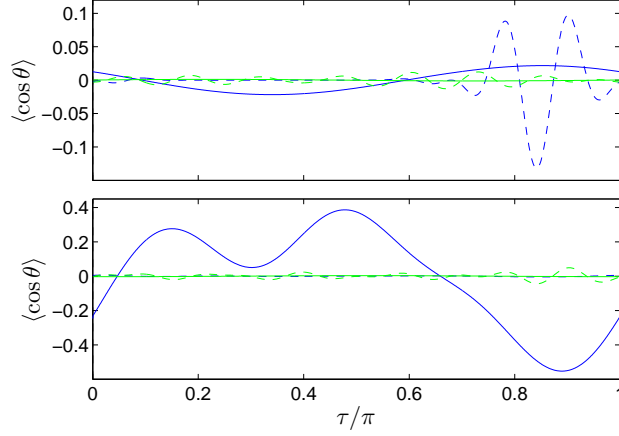


Figure 4: (Color online) Time evolution of $\langle \cos \theta \rangle$ for the cases of Fig. 2 (top panel) and 3 (bottom panel). The same color code as in Fig. 2 and 3 has been used. Solid and dashed lines depict respectively the orientation at $\tilde{T} = 0$ and $\tilde{T} = 50$. The field is on for negative times and switches off at $\tau = 0$. The variable τ is unitless.

level, which consists here in the successive excitation of neighboring rotational levels. This process is efficient only if the field spectrum allows to excite the first rotational frequencies with a sufficient high intensity. Note that this control scheme has already been identified in the literature to produce molecular orientation [15]. The rotational population distribution being displaced to high J levels with increasing temperatures, this mechanism then loses its efficiency very fast. This orientation will be called a *zero-temperature orientation* and can be quantitatively measured by the partial expectation value $\langle \cos \theta \rangle_0$. In the case of an initial thermal distribution of rotational states, a new mechanism occurs. This situation corresponds to molecules with small values of B , i.e. with a quite large frequency F . As can be seen in Fig. 3 for $F = 2.5$, there is no overlap with the population distribution at low temperature and thus no orientation. In this second mechanism at high temperature, the control field excites simultaneously many rotational frequencies (i.e. with a large laser bandwidth), creating several rotational waves packets $|\psi_{J_0, M_0}(t)\rangle$ which interfere constructively to produce a noticeable orientation, denoted *thermal orientation*. This latter can be computed through the expectation value $\langle \cos \theta \rangle_T$. In this scenario, the orientation reaches a maximum at a temperature different from zero and presents a slow decrease with increasing temperatures.

These different conclusions can be checked in Fig. 5 where the zero-temperature and the thermal orientation responses have been plotted. One clearly sees in this figure that the zone (I) is associated to $\langle \cos \theta \rangle_0$, where only the initial state $|0, 0\rangle$ is considered. The efficiency of THz pulses in the region (II) can be interpreted as a thermal orientation such that $\langle \cos \theta \rangle \simeq \langle \cos \theta \rangle_T$. Note that the sum of the two figures 5 does not give exactly the result of Fig. 1 due to destructive interferences between the two orientation responses.

The transition from a regime with thermal orientation to a regime with a zero-temperature orientation can be understood from the definition of the parameters (F, D) . Decreasing the value of B is equivalent to increase the effective frequency F and to decrease the temporal width D of the pulse. Starting from the zone (I) where the spectrum of the field overlaps the first molecular transition, a decrease of the rotational constant B will shift the field spectrum to higher frequencies F . The overlap with the first frequency is removed and no zero temperature orientation is possible. At the same time, as a consequence of the increase of the width of the field spectrum, more and more molecular transitions can be excited by the pulse, leading thus to a thermal orientation.

The evolution of the orientation for the molecules of Table 1 is displayed in Fig. 6. All the molecules considered belong to the zone (I), except for the CO and OCS molecules which present an orientation close to 0 at $T \simeq 0K$ and an orientation of the order of 0.15 and 0.1 at $T \simeq 10K$ and $T \simeq 150K$, respectively. The efficiency of the control scheme at high temperature becomes even better than the one obtained for other molecules such as HF or LiH, which is very good only at low temperature. Note that the CO and LiCl molecules have quite the same parameters F and D . The difference of orientation response comes from the difference of two order of magnitude in their effective amplitude A . A ladder climbing process at $T = 0$ K is possible for LiCl since the tails of the spectrum are sufficient, while it is not the case for CO. The two molecules present however a thermal orientation. We also point out that the orientation of OCS at high temperature is due to its low value of D (very broad spectrum) combined with a high value of F and a large effective amplitude of the field.

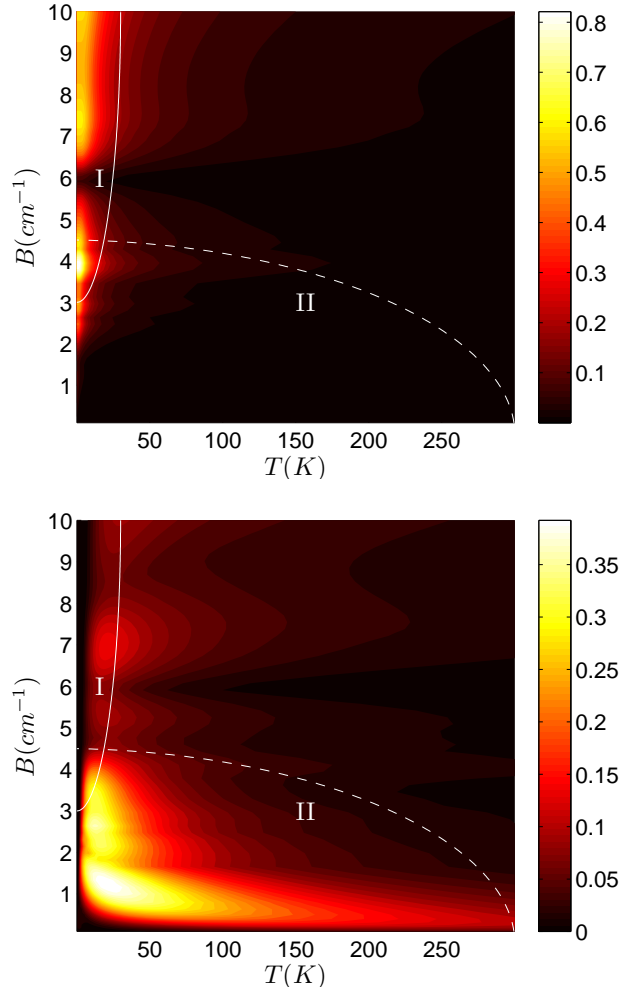


Figure 5: (Color online) Same as Fig. 1 but for the zero temperature contribution $\langle \cos \theta \rangle_0$ to the molecular orientation (top) and for the thermal one $\langle \cos \theta \rangle_T$ (bottom).

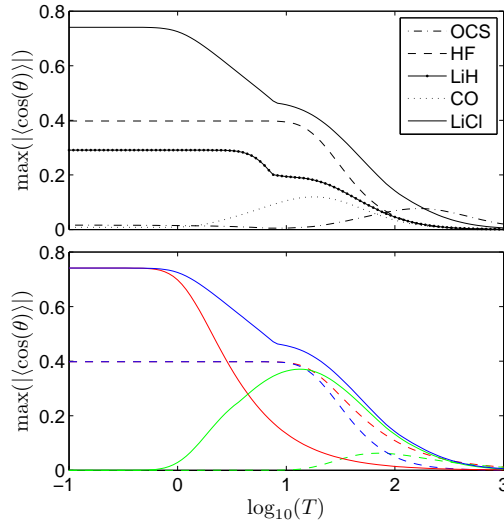


Figure 6: (Color online) The top panel represents the evolution of the maximum of orientation as a function of the temperature for the molecules of Table 1. The field parameters of Fig. 1 have been used. The contribution of the zero temperature (red or dark gray) and thermal (green or light gray) wave packets have been plotted for the LiCl (solid lines) and HF (dashed lines) molecules in the bottom panel. The blue (black) lines corresponds to the total orientation response. The temperature T is expressed in Kelvin.

In Fig. 6, note the smooth evolution of the orientation, except in the cases of the LiH and LiCl molecules where a slope change occurs. This feature can be explained by a transition from a zero-temperature orientation to a thermal one as shown in Fig. 6 (bottom). It can be seen that the non smooth point of the curve for the LiCl molecule can be viewed as a limit point for which the thermal orientation becomes predominant with respect to the zero-temperature one.

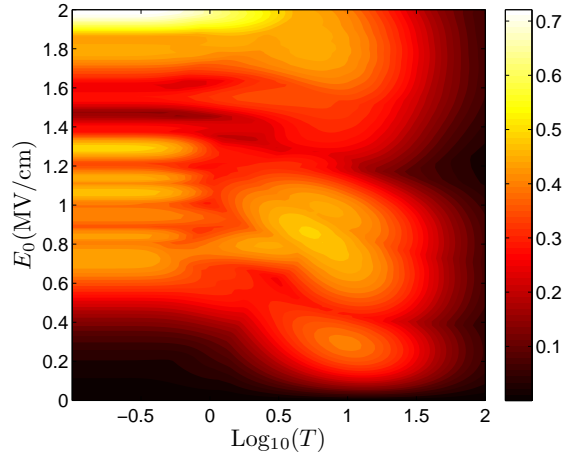


Figure 7: (Color online) Maximum orientation as a function of the field amplitude E_0 and the temperature T . The other field parameters are $\delta = 5$ ps and $f = 0.5$ THz. The LiCl molecule is considered for the computations. The temperature T is expressed in Kelvin.

We finally explore the dependance of the orientation with respect to the field strength. A global description of this sensitivity as a function of the temperature is displayed in Fig. 7. At zero temperature, we observe a quadratic increase of the orientation up to $E_0 \simeq 0.6$ MV/cm. Higher amplitudes lead to a more chaotic evolution of the orientation characterized by the occurrence of maxima and minima. At high temperature, the same erratic distribution of the orientation response can be seen with, however, a larger periodicity. We thus conclude that the molecular orientation is less sensitive to amplitude field changes at non-zero than at zero temperature. We also observe that the thermal orientation can be produced at a lower intensity than the zero temperature one.

4 Conclusion

This paper has focused on the use of THz laser pulses for controlling the orientation dynamics of linear molecules. Numerical tests have shown the efficiency of the proposed control scheme, even at high temperature for some molecules. Until now, most of the works have envisaged the production of molecular orientation with short laser pulses characterized by a non zero time average of the electric field as, e.g., with the use of HCPs. Indeed, the sudden impact approximation predicts no post-pulse orientation when this average vanishes. Opposite to this accepted fact, we have shown that a significant orientation can

be obtained in two different regimes. The first one corresponds to a standard situation with low temperature and high rotational constants. In the second case, for an adequate choice of the pulse parameters, we have established that the temperature plays an active role in the production of molecular orientation. This study calls for further experimental investigation of the use of such laser pulses in order to complete the initial work of Ref. [46]. In particular, one objective could be to demonstrate experimentally the existence of thermal orientation in molecules such that OCS or CO.

Acknowledgment

We are grateful to E. Hertz for discussions.

References

- [1] R. C. C. Brif and H. Rabitz, *New J. Phys.* **12**, 075008 (2010).
- [2] M. Shapiro and P. Brumer, *Principals of quantum control of molecular processes* (Wiley, New York, 2003).
- [3] S. Rice and M. Zhao, *Optimal control of molecular dynamics* (Wiley, New York, 2000).
- [4] H. Stapelfeldt and T. Seideman, *Rev. Mod. Phys.* **75**, 543 (2003).
- [5] T. Seideman and E. Hamilton, *Adv. At. Mol. Opt. Phys.* **52**, 289 (2006).
- [6] B. Friedrich and D. Herschbach, *Phys. Rev. Lett.* **74**, 4623 (1995).
- [7] M. Leibscher, I. S. Averbukh, and H. Rabitz, *Phys. Rev. Lett.* **90**, 213001 (2003).
- [8] S. Zhdanovich, A. A. Milner, C. Bloomquist, J. Flob, I. S. Averbukh, J. W. Hepburn, and V. Milner, *Phys. Rev. Lett.* **107**, 243004 (2011).
- [9] E. Gershnabel and I. S. Averbukh, *Phys. Rev. Lett.* **104**, 153001 (2010).
- [10] M. Z. Hoque, M. Lapert, E. Hertz, F. Billard, D. Sugny, B. Lavorel, and O. Faucher, *Phys. Rev. A* **84**, 013409 (2011).
- [11] M. Lapert, E. Hertz, S. Guérin, and D. Sugny, *Phys. Rev. A* **80**, 051403 (2009).
- [12] D. Sugny and M. Joyeux, *J. Chem. Phys.* **112**, 31 (2000).
- [13] S. Ramakrishna and T. Seideman, *Phys. Rev. Lett.* **95**, 113001 (2005).
- [14] D. Sugny, C. Kontz, and H. Jauslin, *Phys. Rev. A* **74**, 053411 (2006).
- [15] J. Salomon, C. M. Dion, and G. Turinici, *J. Chem. Phys.* **123**, 144310 (2005).
- [16] M. Lapert, R. Tehini, G. Turinici, and D. Sugny, *Phys. Rev. A* **78**, 023408 (2008).
- [17] R. R. Jones, D. You, and P. H. Bucksbaum, *Phys. Rev. Lett.* **70**, 1236 (1993).

- [18] T. Seideman, J. Chem. Phys. **115**, 5965 (2001).
- [19] C. M. Dion, A. Keller, and O. Atabek, Eur. Phys. J. D **14**, 249 (2001).
- [20] N. E. Henriksen, Chem. Phys. Lett. **312**, 196 (1999).
- [21] M. Machholm, J. Chem. Phys. **115**, 10724 (2001).
- [22] C. M. Dion, A. B. Haj-Yedder, E. Cancès, A. Keller, C. L. Bris, and O. Atabek, Phys. Rev. A **65**, 063408 (2002).
- [23] E. Gershnel, I. S. Averbukh, and R. J. Gordon, Phys. Rev. A **74**, 053414 (2006a).
- [24] E. Gershnel, I. S. Averbukh, and R. J. Gordon, Phys. Rev. A **73**, 063402 (2006b).
- [25] D. Daems, S. Guérin, D. Sugny, and H. R. Jauslin, Phys. Rev. Lett. **94**, 153003 (2005).
- [26] S. D. I. Znakovskaya, F. A. D. Ray, N. G. Johnson, I. A. Bocharova, M. Magrakvelidze, B. D. Esry, C. L. Cocke, I. V. Litvinyuk, and M. F. Kling, Phys. Rev. Lett. **103**, 153002 (2009).
- [27] R. Tehini and D. Sugny, Phys. Rev. A **77**, 023407 (2008).
- [28] S. Zhang, C. Lu, T. Jia, Z. Wang, and Z. Sun, Phys. Rev. A **83**, 043410 (2011a).
- [29] R. Tehini, M. Z. Hoque, O. Faucher, and D. Sugny, Phys. Rev. A **85**, 043423 (2012).
- [30] S. Zhang, C. Lu, T. Jia, Z. Wang, and Z. Sun, J. Chem. Phys. **135**, 034301 (2011b).
- [31] S. Zhang, J. Shi, H. Zhang, T. Jia, Z. Wang, and Z. Sun, Phys. Rev. A **83**, 023416 (2011c).
- [32] J. Wu and H. Zeng, Phys. Rev. A **81**, 053401 (2010).
- [33] Y. Hyeok, K. H. Taek, K. C. Min, N. C. Hee, and L. Jongmin, Phys. Rev. A **84**, 065401 (2011).
- [34] I. S. Averbukh and R. Arvieu, Phys. Rev. Lett. **87**, 163601 (2001).
- [35] D. Sugny, A. Keller, O. Atabek, D. Daems, C. M. Dion, S. Guérin, and H. R. Jauslin, Phys. Rev. A **69**, 033402 (2004a).
- [36] D. Sugny, A. Keller, O. Atabek, D. Daems, C. M. Dion, S. Guérin, and H. R. Jauslin, Phys. Rev. A **72**, 032704 (2005a).
- [37] D. Sugny, A. Keller, O. Atabek, D. Daems, C. M. Dion, S. Guérin, and H. R. Jauslin, Phys. Rev. A **71**, 063402 (2005b).
- [38] C.-C. Shu, K.-J. Yuan, W.-H. Hu, J. Yang, and S.-L. Cong, Phys. Rev. A **78**, 055401 (2008).

- [39] J. Ortigoso, arXiv p. 1108.3991 (2011).
- [40] D. Sugny, A. Keller, O. Atabek, D. Daems, S. Guérin, and H. R. Jauslin, Phys. Rev. A **69**, 043407 (2004b).
- [41] D. You and P. H. Bucksbaum, J. Opt. Soc. Am. B **14**, 1651 (1997).
- [42] C.-C. Shu, K.-J. Yuan, W.-H. Hu, and S.-L. Cong, J. Chem. Phys. **132**, 244311 (2010).
- [43] C.-C. Shu, K.-J. Yuan, W.-H. Hu, and S.-L. Cong, Phys. Rev. A **80**, 011401(R) (2009a).
- [44] C.-C. Shu, K.-J. Yuan, W.-H. Hu, and S.-L. Cong, Opt. Lett. **34**, 3190 (2009b).
- [45] C. Qin, Y. Tang, Y. Wang, and B. Zhang, Phys. Rev. A **85**, 053415 (2012).
- [46] S. Fleischer, Y. Zhou, R. W. Field, and K. A. Nelson, Phys. Rev. Lett. **107**, 163603 (2011).
- [47] A. G. Stepanov, L. Bonacina, S. V. Chekalin, , and J.-P. Wolf, Opt. Lett. **33**, 2497 (2008).

